Identification of the Proton Channel to the Active Site Type 2 Cu Center of Nitrite Reductase: Structural and Enzymatic Properties of the His254Phe and Asn90Ser Mutants[†,‡]

Michael A. Hough,[§] Robert R. Eady,[||] and S. Samar Hasnain*[,§]

Molecular Biophysics Group, School of Biological Sciences, University of Liverpool, Liverpool L69 7ZB, U.K., and STFC Daresbury Laboratory, Warrington, Cheshire WA4 4AD, U.K.

Received July 22, 2008; Revised Manuscript Received October 24, 2008

ABSTRACT: Proton and electron delivery to the catalytic site and their associated pathways are crucial elements in understanding the mechanisms of redox enzymes. Two distinct proton channels have previously been identified in copper nitrite reductases based on high- to atomic-resolution crystal structures. These were assigned as the "primary" and "high-pH" proton channels and link the catalytic type 2 Cu center to the enzyme surface. Residue His254 has been identified as a key residue in the primary proton channel from the catalytic T2Cu site to the surface, while Asn90 is thought to be a key residue in the high-pH channel. The structure of the His254Phe mutant was previously determined to 1.85 Å resolution, revealing disruption in the H-bonding network of the primary proton channel. The effect of the mutation on proton transfer was not established as the T2Cu center was unusually occupied by Zn. New growth protocols have now led to the incorporation of copper at this site, and here we present spectroscopic, catalytic activity, and structural data for the Cu-loaded H254F mutant of *Ax*NiR. Surprisingly, this species exhibits essentially full catalytic activity, despite the clear disruption of the primary proton channel. In contrast, the Asn90Ser mutation disrupts H-bonding in the high-pH proton channel and results in an ~70% decrease in specific activity. These mutations do not change the apparent K_m for nitrite, and thus, these data clearly demonstrate a role for the high-pH proton channel in the delivery of protons to the catalytic T2Cu center at physiological pH values; it may in fact be the main source of protons to the T2Cu center.

In the denitrification process, microbes remove fixed nitrogen from the biosphere by the sequential reduction of nitrate to N_2 via the intermediates nitrite, NO, and N_2O. This is a process of agronomic, environmental, and medical importance (*1, 2*). Copper-containing nitrite reductases (CuNiRs) catalyze the first committed step in the denitrification process of the geo-biological nitrogen cycle ($NO_2^- + 2H^+ + e^- \rightarrow NO + H_2O$), a reaction leading to the formation of the gaseous product NO. These enzymes are trimers of 106 kDa with each monomer having two domains with a characteristic β-sandwich motif. Each monomer contains a buried type 1 Cu (T1Cu)[1] center with ($Cys \cdot Met \cdot His_2$) ligation and a type 2 Cu (T2Cu) site with ($His_3 \cdot H_2O$) ligation at the interface between two monomers, both of which provide the T2Cu ligands. During enzyme turnover, the T1Cu center accepts electrons from the putative physiological electron donors azurin and pseudoazurin, which are then transferred to the T2Cu center where nitrite reduction occurs. The binding of nitrite to the oxidized T2Cu center and the subsequent electron transfer reaction have been the subject of intensive study (*2*−*6*), but the mechanism(s) of proton transfer remains poorly understood. It was proposed, on the basis of the crystal structure of *Alcaligenes xylosoxidans* nitrite reductase (*Ax*NiR) at pH 4.6, that proton transfer occurs from the enzyme surface to the T2Cu center via a well-ordered, hydrogen-bonded water network (*7*), henceforth termed the primary proton channel. This channel extends along the monomer−monomer interface, connecting residue Asp92 at the T2Cu site to the protein surface via residue His254 that was proposed to regulate proton flow. In a later crystal structure at pH 8.5, a second proton channel was identified (*8*), connecting Asp92 to the surface via residues Ala131, Asn90, and Asn107 and several water molecules (termed the high-pH channel). Henceforth, the "high-pH" or "secondary proton channel" refers to this channel, originally observed in a structure determined at pH 8.5. Subsequently, the very high resolution 1.04 Å resolution structure of *Ax*NiR, determined at pH 6.5, showed that both networks are present (*9*). These networks are conserved among different NiRs since they were also observed in the recent atomic-resolution structures of the green nitrite reductase from *Achromobacter cycloclastes* (*3*), where the

[†] The authors gratefully acknowledge support from BBSRC (Grant BBD0162901 to S.S.H. and R.R.E.) and provision of facilities at STFC Daresbury Laboratory.

[‡] Coordinates and structure factors have been deposited in the RCSB Protein Data Bank as entries 2JL3 (H254F) and 2JL0 (N90S).

* To whom correspondence should be addressed. E-mail: s.s.hasnain@liverpool.ac.uk. Phone: +44 151 795 5149. Fax: +44 192 560 3748.

[§] University of Liverpool.

[||] STFC Daresbury Laboratory.

[1] Abbreviations: T1Cu, type 1 copper; T2Cu, type 2 copper; NiR, nitrite reductase; *Ac*NiR, *Achromobacter cycloclastes* nitrite reductase; *Ax*NiR, *Alcaligenes xylosoxidans* nitrite reductase; *Af*NiR, *Alcaligenes facaelis* nitrite reductase; EPR, electron paramagnetic resonance; PEG 550 MME, polyethylene glycol 550 monomethyl ether; rms, root-mean-square.

10.1021/bi801369y CCC: $40.75
Published on Web 11/24/2008

two positions adopted by Asp92 in the resting and substrate-bound forms of the enzyme were also apparent.

To probe the role of the primary proton channel, we previously constructed the His254Phe mutant of *Ax*NiR and showed that enzymatic activity was lost (*10*). However, structural analysis of the mutant enzyme showed the T2Cu center to be occupied by Zn rather than Cu (henceforth termed Zn-H254F), and as a result, the effect of the mutation could not be directly addressed, as T2Cu is essential for nitrite reductase activity. Our previous attempts to incorporate copper into the T2Cu center in this mutant failed, and this has remained a frustrating aspect of attempts to define proton uptake events in NiR.

Here, we describe a form of the H254F mutant of *Ax*NiR, purified using a modified protocol that resulted in a high level of Cu occupancy at the T2Cu center (henceforth termed Cu-H254F). The specific activity of this mutant enzyme when normalized for the T2Cu occupancy is comparable to that of the wild-type enzyme, indicating that efficient proton transfer is able to occur despite the clear disruption of the primary proton channel, as confirmed by the crystal structure of this Cu-H254F mutant to 1.5 Å resolution. These data suggest that the secondary proton channel, previously thought to be active only at high pH, is operative at physiological pH and is sufficient to maintain essentially full enzymatic activity. This is confirmed by our structural (1.6 Å resolution) and biochemical characterization of the Asn90Ser *Ax*NiR mutant where H-bonding in the high-pH proton channel is disrupted and an ~70% reduction in specific activity is observed.

EXPERIMENTAL PROCEDURES

Protein Production. Recombinant mutant H254F and N90S *Ax*NiR were produced using a protocol modified from that described previously (*10*). Cells were grown in LB medium supplemented with 1 mM $CuSO_4$ immediately before induction with IPTG. Following cell lysis and centrifugation, the supernatant containing mutant *Ax*NiR was further dialyzed against 1 mM $CuSO_4$ and 20 mM MES (pH 6) prior to chromatographic purification on carboxymethyl-cellulose as described previously (*11*). Crystals were grown using the hanging drop vapor diffusion method at 20 °C. Three microliters of a protein solution at 10 mg/mL in 20 mM Tris-HCl (pH 7.4) was mixed with an equal volume of reservoir solution containing 15−20% PEG 550 MME, 10 mM $ZnSO_4$, and 100 mM MES (pH 6.5). Crystals in space group *R*3 grew within 1 week and were an intense blue color. In situ single-crystal optical spectroscopy (*12*) indicated that the frozen T1Cu center was in the oxidized, Cu(II) form prior to X-ray data collection for both mutants.

EPR and UV−Visible Spectroscopy. X-Band EPR spectra were collected at 143 K using a JEOL FES-RE2X spectrometer fitted with a JEOL microwave bridge and a JEOL DVT2 temperature controller. The microwave frequency was 9.125 GHz (Cu-H254F) or 9.13 GHz (N90S), and the microwave power was 4 mW. The modulation width was 1 mT and the time constant 0.1 s. The spectra for the type 1 and type 2 Cu centers were simulated using the in-house software EiBook8 (R. W. Strange, personal communication) (Table 1). UV−visible spectra were recorded using a Perkin-Elmer Lambda 35 or Lambda 16 spectrophotometer. An extinction coefficient of 1.54 M^{-1} cm^{-1} was used to estimate protein concentration.

Table 1: EPR Simulation Parameters for Cu-H254F, Zn-H254F, N90S, and Recombinant Native *Ax*NiR

	Cu-H254F	Zn-H254F[a]	N90S	recombinant native[b]
type 1 Cu				
g_x, g_y	2.055	2.04	2.05	2.05
A_x, A_y (mT)	0	0.5	2.05	0
g_z	2.225	2.23	2.235	2.24
A_z (mT)	6.0	6.0	6.0	6.3
type 2 Cu				
g_x, g_y	2.055	−	2.055	2.05
A_x, A_y (mT)	0	−	0	0
g_z	2.33	−	2.35	2.38
A_z (mT)	13.0	−	11.0	12.7

[a] No T2Cu signal was present in the Zn-H254F EPR spectrum. [b] Parameters taken from ref *12*.

Table 2: Kinetic Parameters for Native and Mutant *Ax*NiR

	specific activity	apparent K_m for nitrite (μM)	ref
wild-type *Ax*NiR	240[a]	34	*20*
H254F	123 (246[b])	50	this work
N90S	82	50	this work

[a] Specific activity of recombinant native *Ax*NiR prepared using a protocol identical to that used for the mutants. [b] Specific activity scaled to a T2Cu content of 50%.

Enzyme Activity Assays. The discontinuous methyl viologen assay was performed as described previously (*13*). One unit of activity was defined as the reduction of 1 μmol of nitrite per minute per milligram of protein. This standard assay for NiR utilizes a stopped-time reaction followed by the colorimetric estimation of the amount of nitrite remaining in the reaction mixture. Because of the high affinity of Cu-NiR for nitrite, this makes the determination of the apparent K_m for nitrite using this method technically challenging. In this study, the NO_2^- concentration ranged from 5 to 200 μM, and for each concentration, a time course (typically from 30 s to 4 min) was performed to ensure that initial rates of reaction were determined. In addition, at the lower NO_2^- concentration, the volume of the reaction mixture analyzed for residual nitrite was increased to yield reliable absorbance measurements. The data are summarized in Table 2. Assays using the physiological redox partner azurin were performed as described previously (*12*). Reduced azurin I was prepared in an anaerobic glovebox. The degassed assay reaction mixture contained 22.5 μM reduced azurin I and 20 mM sodium nitrite in 100 mM Tris-HCl (pH 7.1). The reaction was performed under nitrogen and was initiated via the injection of NiR through the rubber seal of the cuvette. The low rate of oxidation of azurin I in the absence of enzyme was determined in a blank assay using water instead of a protein solution, and this slope was subtracted from that obtained in the protein assays. One unit of enzyme activity is defined as the oxidation of 1 μmol of azurin per minute per milligram of NiR.

Crystallographic Data Collection. Crystals were transferred into a cryoprotectant solution consisting of reservoir solution with a PEG 550 MME concentration of 30−35% before being frozen to 100 K in a nitrogen cryostream. Crystallographic data were measured to 1.5 Å (Cu-H254F) and 1.6 Å (N90S) resolution on SRS beamline 10 (*14*) at an

Table 3: Data Collection, Refinement, and Model Statistics

	Cu-H254F	N90S
Data Collection		
space group	*R*3	*R*3
cell dimensions *a*, *b*, *c* (Å)	89.3, 89.3, 287.9	89.6, 89.6, 287.7
resolution (Å)	26.0−1.50	29−1.60
R_{merge}	0.048 (0.27)[a]	0.072 (0.329)[a]
$I/\sigma(I)$	18.9 (2.95)[a]	12.0 (2.10)[a]
completeness (%)	97.1 (78.2)[a]	93.8 (60.6)[a]
Wilson *B* factor (Å^2)	25	19
Refinement		
R_{work}	0.174	0.193
R_{free}	0.198	0.222
ESU (Å)	0.06	0.09
no. of protein atoms	5033	5173
no. of water molecules	658	602
average *B* factor (Å^2)		
protein	22.6	17.8
water	32.9	26.1
root-mean-square deviation		
bond lengths (Å)	0.015	0.015
bond angles (Å)	1.75	1.77
Ramachandran plot		
most favored (%)	97.4	96.7
PDB entry	to be added	to be added

[a] Values in parentheses are for the outer-resolution shell.

X-ray wavelength of 0.98 Å using a MAR 225 CCD detector. Data were processed using HKL2000, and the structure was determined by molecular replacement in PHASER (*15*) in the CCP4 program suite with the 1.04 Å resolution structure of *Ax*NiR in space group $P6_3$ (*9*) (PDB entry 1oe1) as the search model. Water molecules and double conformations were removed from the model prior to structure solution. The structures were refined using REFMAC5 (*16*) in the CCP4 program suite. At maximum resolution, riding hydrogens were added to the model and TLS parameters (*17*) for each of the two monomers refined. Rebuilding of the model between refinement cycles was performed in Coot (*18*). Water molecules were added using ARP/WARP and by manual methods. The models were assessed using PROCHECK (*19*) and Coot (*18*). A summary of the data and refinement statistics and the quality indicators for the structures is given in Table 3. Anomalous data were collected from the same crystals at a wavelength of 1.33 Å using SRS beamline 10 to identify the proportion of Cu present at each site.

RESULTS

The Cu ion of the T2Cu center of both wild-type and recombinant *Ax*NiR is readily lost on disruption of the bacterial cells. To minimize this loss, crude cell extracts are routinely dialyzed against buffers containing 1 mM $CuSO_4$ (*13*). In the case of the H254F variant, these conditions are not sufficient to populate the type 2 active site with Cu (*10*). To increase the Cu occupancy, we modified the growth conditions to increase the Cu content of the medium to 1 mM $CuSO_4$. Preparations of mutated *Ax*NiR from these cells indicated that this change did promote the incorporation of Cu into the T2Cu site, enabling us to provide definitive results on the potential significance of the "primary proton channel" in proton transfer. To complement this study, we also used this procedure to purify *Ax*NiR with Asn90 mutated to Ser to potentially disrupt H-bonding in the so-called high-pH proton channel.

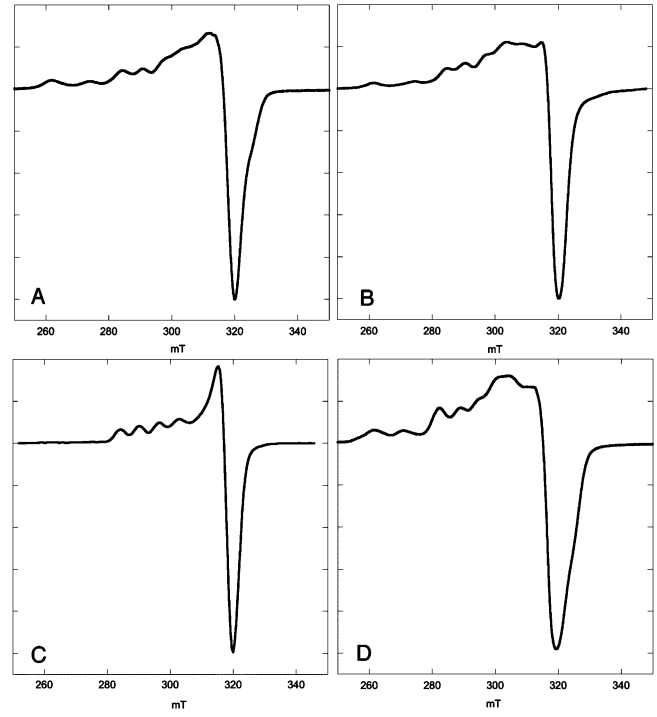

FIGURE 1: EPR spectra of (A) recombinant native *Ax*NiR, (B) Cu-H254F, (C) Zn-H254F, and (D) N90S. For plots A, B, and D, the spectra are a composite of those arising from the T1Cu and T2Cu centers, indicating that a significant level of $T2Cu^{2+}$ is present, with a nearly full level of $T2Cu^{2+}$ in the N90S mutant. The spectrum of Zn-H254F showed that only a T1Cu signal was present.

Electron Paramagnetic Resonance (EPR) Spectroscopy. The X-band EPR spectra of the Cu-H254F and N90S mutants of *Ax*NiR contain contributions from both T1 and T2Cu centers (Figure 1), indicating clearly the presence of Cu in the Cu(II) oxidation state in the T2Cu sites in the mutant enzymes. This is in contrast to the previous study of H254F in which no T2Cu EPR signal was apparent (*10*) and in which the site was demonstrated by anomalous diffraction data to be occupied by Zn. The simulation for Cu-H254F determined that the T1Cu site has an axial spectrum with the following values: $g_\perp = 2.055$, $g_z = 2.225$, and $A_z = 6$ mT. These values are very similar to those obtained for the T1Cu site of native *Ax*NiR (*11*) and for the Zn-H254F preparation (Table 1). Simulation of the T2Cu parameters gave a $g_\perp$ of 2.055, a g_z of 2.33, and an A_z of 13 mT, indicating only a minor change at the T2Cu center in the mutant enzyme compared to the native enzyme. The EPR spectrum of the N90S mutant exhibited strong T2Cu features, indicating that the mutant was essentially fully loaded with Cu in the Cu(II) oxidation state. The simulations gave the following parameters: $g_\perp = 2.05$, $g_z = 2.235$, and $A_z = 6$ mT for the T1Cu center and $g_\perp = 2.055$, $g_z = 2.35$, and $A_z = 11$ mT for the T2Cu center. The small differences in the spectra shown in Figure 1 and Table 1 are within the variation observed in preparations of native *Ax*NiR (*13*) presumed to arise from some heterogeneity of the T2Cu sites.

Activity Measurements. The enzymatic activities of the mutant enyzmes were determined using two methods, using either dithionite with methyl viologen or the physiological donor azurin as the electron donor (*11, 13*). The activity of *Ax*NiR with azurin is some 5-fold lower than that with the artificial electron donors and potentially allows a slower rate of proton delivery (as might be expected from mutation of

Table 4: Cu−Ligand Parameters at the T1Cu Site of *Ax*NiR Structures

	Cu-H254F (A/B)	Zn-H254F	N90S (A/B)	native (1.04 Å)[a]	native (2.1 Å)
T1Cu−His89 $N^{\delta 1}$	2.03/2.05	2.2	2.12/2.08	2.02	2.0
T1Cu−His139 $N^{\delta 1}$	2.01/2.07	2.1	2.17/2.06	2.03	2.0
T1Cu−Cys130 S^{γ}	2.16/2.20	2.2	2.24/2.10	2.20	2.2
T1Cu−Met144 S^{δ}	2.61/2.60	2.6	2.61/2.62	2.45/4.26[a]	2.7

[a] In the 1.04 Å structure of recombinant native *Ax*NiR, the axial methionine ligand is observed in two conformations.

the proton channels) to retain full catalytic activity. However, specific activity measurements (Table 2) using both assay systems revealed that the Cu-H254F activity was ~50% of that of the native enzyme and consistent with the observed partial occupancy (see below) of Cu in the T2 site, indicating that this mutation does not significantly affect catalysis. In contrast, the N90S mutant had a catalytic activity ~70% lower than that of the native enzyme in both assay systems, despite essentially full occupancy of Cu at the T2Cu site. The apparent K_m for NO_2^- for a variety of CuNiRs ranges from 35 to 74 μM. In this study, the values of ~50 μM determined for the H254F and N90S mutants of *Ax*NiR (see Table 2) show that these mutations have not significantly altered the affinity of the enzyme for nitrite, and thus, it is highly likely that the 70% decrease in specific activity of the N90S substitution arises from the disruption of the proton channel from the active site type 2 Cu to the enzyme surface as revealed in the crystal structure, These data suggest that disruption of the high-pH proton channel decreases the effectiveness of proton transfer with a consequent effect on activity.

Crystal Structures of Cu-H254F and N90S AxNiR. The structure of the Cu-loaded H254F *Ax*NiR mutant is determined to 1.5 Å resolution in space group *R*3 with two monomers in the crystallographic asymmetric unit, in contrast to the Zn-occupied T2Cu H254F variant (Zn-H254F) previously determined to 1.85 Å resolution in space group $P6_3$ (*10*). The structure is refined to an *R* factor of 0.174 (R_{free} = 0.198), with an estimated standard uncertainty (ESU) of 0.065 Å (Table 3). The model contains a total of 5033 protein atoms, two PEG molecules, two MES molecules, four Cu ions,[2] and four Zn ions. The Cu-H254F and Zn-H254F variants are essentially structurally identical. The rms deviations in Cα positions following superposition of the two structures were 0.21 Å for monomer A and 0.20 Å for monomer B. A similar superposition with the 1.04 Å native enzyme structure gave a rms deviation of 0.22 Å for both monomers. The Cu-H254F model contains 658 water molecules in contrast to the 236 that were present in the lower-resolution Zn-H254F structure, thus providing a significantly better solvent model.

The N90S structure is determined to 1.6 Å resolution, and the model contains 5173 protein atoms, 602 water molecules, two PEG and two MES molecules, and four Cu[2] and two Zn ions. Superposition of the structure with the native (PDB entry 1oe1) structure shows a rms deviation of 0.26 Å for Cα atoms. In both structures, a surface Zn ion is present in each monomer, bridging the two *Ax*NiR monomers through the coordinating residues His165 and Asp167 of one monomer and Glu195 of the adjacent monomer. This Zn site is similar to that described previously in several *Ax*NiR structures (*10, 12*). A MES buffer molecule is also bound to the protein surface near this point, interacting with the amide nitrogen of His165.

Anomalous Diffraction Data. To discriminate between Cu and Zn ions present at the T2Cu site of H254F and N90S *Ax*NiR crystals, additional data were collected using 1.33 Å (above the Cu K-edge) X-rays. The crystal used for the 1.5 Å resolution structure of Cu-H254F gave peaks in the anomalous map of ~28σ for the T1Cu center and ~8.5σ for the T2Cu center (ratio of 3.3:1) at 1.33 Å. This is indicative of a partial but significant (30−35%) Cu loading at the T2Cu site in the crystal. Subsequent screening of a number of Cu-H254F crystals from the same preparation showed a variable T1Cu:T2Cu ratio of anomalous peaks with the highest T2Cu being 70% of T1Cu and the lowest being 30%. For N90S, the anomalous peaks for T1 and T2Cu were 15σ and 12σ (1.33 Å), respectively, indicating a high occupancy of T2Cu, consistent with the EPR data.

Type 1 Copper Center. The geometries of the T1 and T2 Cu centers are largely unchanged as a result of the mutations (Table 4). The T1Cu center has typical Cu−ligand distances for *Ax*NiR, indicating that the mutations have little effect upon the T1 center. The Cu−Cys130 distances for Cu-H254F are ~2.16 Å (monomer A) and 2.21 Å (monomer B), which are typical of a partially reduced T1 center (*5*), while in N90S, these distances are 2.24 (A) and 2.10 Å (B), respectively, which suggests a different oxidation state of Cu in the two monomers. The optical spectrum of single crystals taken from the same drop as the crystals used for X-ray data collection clearly showed the intense 590 nm peak prior to X-ray exposure, confirming the redox status of the T1Cu center as Cu^{2+}. As has been shown recently (*12*), the T1Cu center can photoreduce readily during X-ray data collection. The earlier 1.85 Å resolution Zn-H254F structure showed small differences in the T1Cu center in comparison to the 2.1 Å structure of the native enzyme (*7*). A 0.15 Å reduction in the Cu−Met144 S^{δ} distance and a 0.15 Å increase in the Cu−His89 $N^{\delta 1}$ distance were observed. However, in the Cu-H254F case, the Cu−ligand distances at the T1Cu center are very similar to those in the more recent 1.04 Å resolution structure of recombinant native *Ax*NiR (*9*) (Table 4), and we consider that the previously observed changes (specifically a shift of 0.15 Å in the Cu−His89 $N^{\delta 1}$ distance) were most likely the result of the limited resolution of the Zn-H254F and native structures. The N90S T1Cu sites closely resemble those of native *Ax*NiR.

The T2Cu center of Cu-H254F has been modeled at full occupancy with a mixture of 0.3 Cu and 0.7 Zn ion, in proportion estimated from the anomalous data for this

[2] The model contains two NiR monomers per asymmetric unit. Each T2Cu center has been modeled with a full-occupancy T1Cu and T2Cu ion, for a total Cu content of six per trimer. The N90S structure contains two zinc ions located at the protein surface. These are also present in the H254F structure as well as two partial-occupancy Zn ions at the T2Cu center for a total of four Zn ions.

Table 5: Cu−Ligand Parameters for the T2Cu Catalytic Centers of *Ax*NiR Structures

	Cu-H254F (Cu A/B)	Cu-H254F (Zn A/B)	Zn-H254F	N90S (A/B)	native (1.04 Å)	native (2.1 Å)
T2Cu[a]−His94 $N^{\varepsilon 2}$	1.89/1.86	2.07/2.13	2.0	2.06/2.08	1.96	2.0
T2Cu−His129 $N^{\varepsilon 2}$	2.26/2.21	1.94/1.89	2.0	2.01/2.07	2.00	2.0
T2Cu−His300 $N^{\varepsilon 2}$	2.18/2.14	2.04/2.06	2.1	2.07/2.12	2.00	2.3
T2Cu/Zn−water	1.82/1.80	2.07/1.94	2.1	1.94/2.23	1.98	1.7
T2Cu/Zn−His24 $9N^{\varepsilon 2}$	3.42/3.51	3.79/3.86	3.7	3.91/3.77	3.74	3.6
Asp92 $O^{\delta 2}$−water	2.57/2.63	2.07/2.63	2.7	2.58/2.41	2.54	2.5

[a] Or Zn, as appropriate.

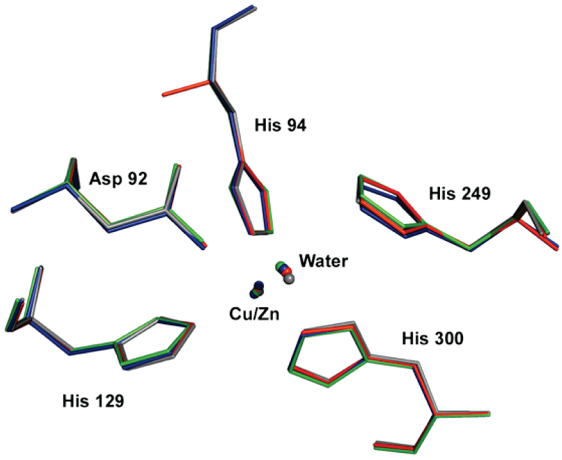

FIGURE 2: Superposition of the T2Cu sites of Cu-H254F (blue), Zn-H254F (gray, PDB entry 1gs7), N90S (green), and native *Ax*NiR (red, PDB entry 1oe1).

particular crystal. The Cu and Zn ions refine to positions ~0.2 Å apart. A full-occupancy water molecule is present, ligated to the ion(s) occupying the T2Cu center at distances of ~1.9 Å (to Cu) and ~2.0 Å (to Zn). For N90S, a full-occupancy Cu ion was modeled at the site. Metal−ligand bond distances are given in Table 5 and compared with those for Zn-H254F and recombinant native *Ax*NiR. The superposition of the structures in the T2Cu region is shown in Figure 2.

Proton Channels and H254F and N90S Mutations. (i) H254F Mutation. The mutation of His254 to Phe is confirmed by the 1.5 Å resolution electron density (Figure 3a). The organizational arrangement of the primary proton channel is very similar to that observed in the Zn-H254F structure. The H-bonding network present in the native structure is only partially present in the mutant enzyme. The T2Cu-coordinated water molecule is H-bonded to Asp92, which in turn is H-bonded to a water molecule in the channel (W2). This water bonds to another water molecule (W3) that, in the native structure, is H-bonded to His254 $N^{\varepsilon 2}$. In the absence of this H-bond in the mutant, the electron density for this water is elongated, indicating a spread of positions, toward the aromatic ring of Phe254, which is in a perpendicular orientation with respect to the channel. The water molecule (W4) that in the native structure is H-bonded to the second side chain $N^{\delta 1}$ atom of His254, in the mutant is shifted by 2.2 Å toward Lys290. The loss of the two His254−water H-bonds clearly disrupts the proton channel such that proton transfer can no longer occur through this route. The high-pH proton channel (Asp92−water−water−Ala131−Asn90−Asn107) from the T2Cu site to the protein surface, as identified in the high-pH and atomic-resolution structures of *Ax*NiR, is clearly present in the Cu-H254F structure (Figure 3b). It is likely that proton delivery

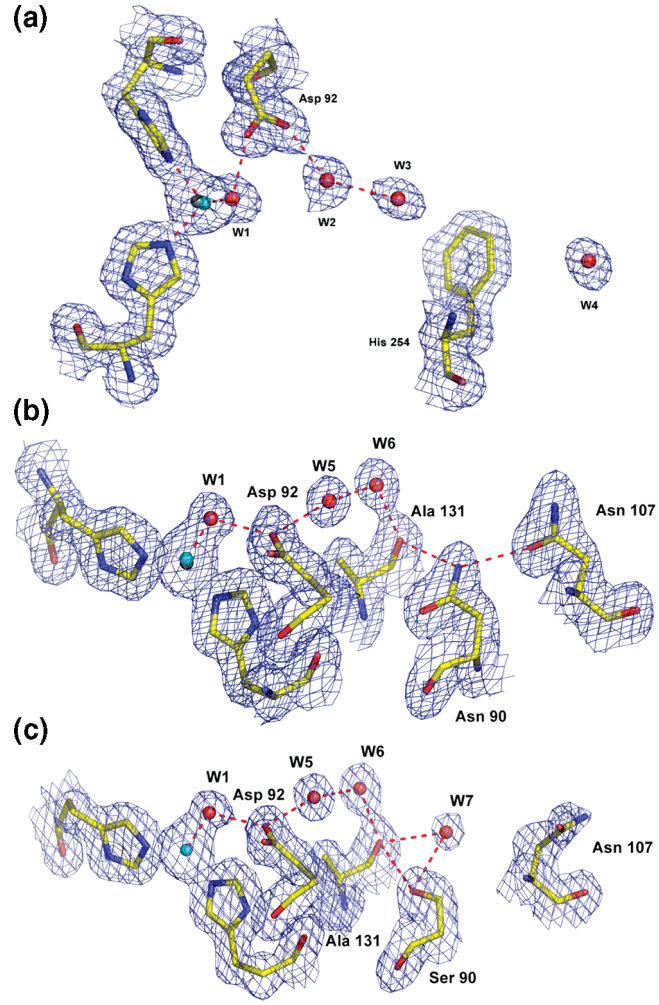

FIGURE 3: $2F_o - F_c$ electron density maps, contoured at 1σ, showing the hydrogen-bonding networks (proton channels). The Cu ion is shown as a cyan sphere, while the Zn ion is colored gray. (a) Primary proton channel and His254Phe mutation site in the Cu-H254F structure. The loss of two hydrogen bonds from residue His254 on mutation to Phe effectively destroys the hydrogen bonding network proposed to be the primary proton channel. (b) High-pH proton channel from T2Cu to the protein surface in Cu-H254F via residues 90, 92, 107, and 131 and several conserved water molecules. This channel is intact in the Cu-H254F mutant. (c) High-pH proton channel in the N90S mutant. The mutation removes the Asn90−Asn107 hydrogen bond, and an additional water molecule is bound to Ser90 $O^{\gamma 1}$.

in the H254F mutant takes place via this so-called "secondary" or high-pH pathway for the enzyme to be able to exhibit activity at physiological pH.

(ii) N90S Mutation. The N90S crystal structure clearly shows the truncation of the side chain of residue 90 to serine (Figure 3c). As a consequence of the mutation, the adjacent strand containing Ala131 shifts toward residue 90 such that the hydrogen bond between Asn90 $N^{\delta 1}$ and Ala131 O in the

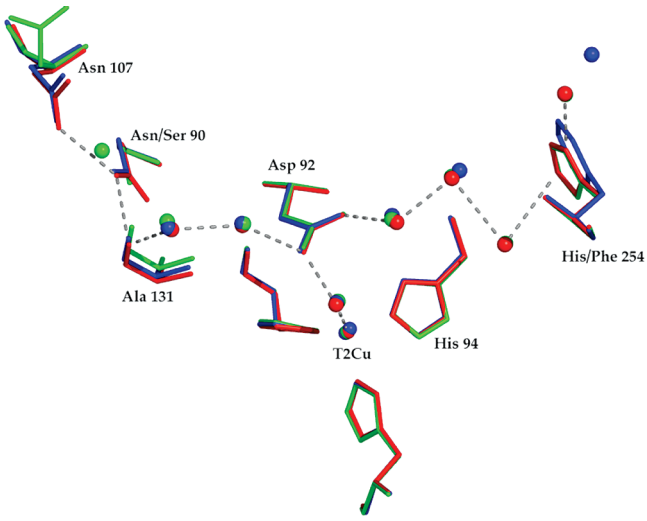

FIGURE 4: Superposition of the proton channels in Cu-H254F (blue), N90S (green), and recombinant native *Ax*NiR (red). In Cu-H254F, only the high-pH channel is intact, while in N90S, only the primary channel is intact. Hydrogen bonds involved in the proton channels in native *Ax*NiR are shown as gray dashed lines.

native protein is replaced with a H-bond between Ser90 $O^{\gamma 1}$ and Ala131 O in the N90S mutant. Crucially, the mutation also results in the loss of the Asn90−Asn107 H-bond (the distance between Ser90 $O^{\gamma 1}$ and the Asn107 native position is >3.8 Å). The side chain of Asn107 displays significant disorder as a result of the loss of its stabilizing hydrogen bond and moves to a new orientation pointing out into the bulk solvent.[3] The mutation therefore clearly disrupts the H-bonding network in the high-pH channel. An additional water molecule, not present in the native *Ax*NiR structure, is observed in the N90S structure, hydrogen bonded to the $O^{\gamma 1}$ atom of Ser90. A superposition of the N90S, Cu-H254F, and 1.04 Å native structures in the region of the primary and high-pH proton channels is shown in Figure 4.

DISCUSSION

Proton Channels and Catalytic Activity. The Cu-H254F structure confirms the observation, originally made on the basis of the lower-resolution Zn-H254F structure, that the His → Phe mutation at position 254 disrupts the proposed primary proton channel due to the loss of two hydrogen bonds involving His254. The catalytic activity of Cu-H254F (allowing for differences in the Cu occupancy of the T2Cu site) and apparent K_m for nitrite are similar to those of the native enzyme, whether using an artificial (methyl viologen) or a physiological (azurin) electron donor. Thus, this substitution that disrupts the so-called primary proton channel (see below) has no significant effect on the catalytic efficiency of *Ax*NiR, indicating that protons must be able to be delivered through alternative routes.

The higher resolution of the current structure also reveals the high-pH water channel (originally observed at high pH but which has been subsequently observed in all of the high-resolution (1.5 Å) and atomic-resolution structures of *Ax*NiR as well as in the high- and atomic-resolution structures of *Ac*NiR and *Af*NiR). In these green CuNiRs, however, Asn107[4] is substituted with Glu (*Af*NiR) or Gln (*Ac*NiR) in an orientation where the side chain points away from Asn90. In these cases, the high-pH proton channel may instead be continued through an ~3.0 Å hydrogen bond between Asn90 and the carbonyl of a glycine residue (Gly109 in both *Af*NiR and *Ac*NiR, the equivalent of Ala103 in *Ax*NiR) and hence to bulk solvent (Figure S1 of the Supporting Information). Due to the altered conformation of Asn90 and the presence of glycine at position 109 in green NiRs, the equivalent Asn90−Ala103 distance in *Ax*NiR is 3.6 Å.

The N90S mutation in *Ax*NiR has no effect on the apparent K_m for nitrite but does result in an ~70% decrease in specific activity, indicating the importance of the high-pH proton channel for NiR activity. The structure reveals that the mutation results in disruption of the high-pH channel due to the change in the hydrogen bonding network involving Asn90 and loss of the bond between Asn90 and Asn107. The remaining catalytic activity of the N90S mutant enzyme indicates that proton transfer, required for enzyme turnover, still occurs but with a lower efficiency than in the native enzyme or the Cu-H254F mutant. Protons could be transferred through the primary proton channel, but it is also possible that protons are able to pass though the high-pH channel despite the mutation of N90 to serine. W7 that is H-bonded to Ser90 O^{γ} may be able to transfer protons from bulk solvent, albeit less efficiently than via the Asn90−Asn107 pathway. Residue Asn90 appears to be crucial for the high-pH proton channel in blue and green NiRs, although the final protein residue involved may differ (Gly109 in green NiRs rather than Asn107 in *Ax*NiR; see the Supporting Information). We note the residual activity of the N90S mutant indicates that protons are not delivered via Ala103 as the Ser90 O−Ala103 O distance is >4.0 Å in the mutant structure.

Taken together, these data for the Cu-H254F and N90S mutants indicate that (i) the high-pH proton channel is able to efficiently supply protons to the T2Cu site and remain operative at physiological pH (the structures were determined at pH 6.5, while the assays were performed at pH 7.1) and (ii) disruption of the high-pH channel results in a severely diminished catalytic activity even when the primary proton channel is intact. These data therefore indicate that the high-pH channel is in fact more important than originally perceived. It may in fact be the main source of protons to the catalytic T2Cu site of CuNiRs, although it remains possible that the primary proton channel also provides a supportive role. In conclusion, the H254F mutant of *Ax*NiR has been produced via a modified growth and purification protocol resulting in the partial incorporation of T2Cu, in contrast to the previously reported structure where Zn was present only at the T2 site. This mutant retains a significant level of catalytic activity commensurate with the T2Cu occupancy despite disruption of the primary proton channel, as confirmed by the 1.5 Å resolution crystal structure. The high-pH proton channel is clearly present and intact in the crystal structure, thus providing a rationale for the activity of the mutant. The N90S mutant shows a greatly reduced

[3] The side chain of Asn107 was modeled with an occupancy of 0.5 in monomer A of the N90S structure. In monomer B, the electron density was weak and the side chain was not modeled.

[4] The numbering is that of the equivalent residues in *Ax*NiR. For the residues discussed here, residue numbering is +6 in the green NiRs such that Asn90 (*Ax*NiR) is equivalent to Asn96 (*Af*NiR and *Ac*NiR).

catalytic activity in comparison to that of native *Ax*NiR, and the structure clearly shows disruption of the high-pH channel due to the loss of the hydrogen bonding involving Asn90. Taken together, these data indicate that the primary proton channel is not essential for efficient catalysis in Cu nitrite reductase and that the high-pH proton channel is effective for proton transfer and operative at physiological pH. This suggests that the high-pH proton channel may be the main source of protons to the T2Cu site. These data thus provide new insights into the critical proton transfer pathways in Cu nitrite reductases.

ACKNOWLEDGMENT

We acknowledge Dr. Richard Strange of the University of Liverpool and Dr. Mark Ellis of STFC Daresbury Laboratory for their help and interest.

SUPPORTING INFORMATION AVAILABLE

A figure showing the superposition of high-pH proton channel residues in *Ax*NiR, *Ac*NiR, and *Af*NiR. This material is available free of charge via the Internet at http://pubs.acs.org.

REFERENCES

1. Zumft, W. G. (1997) Cell biology and the molecular basis of denitrification. *Microbiol. Mol. Biol. Rev. 61*, 533–616.
2. Eady, R. R., and Hasnain, S. S. (2003) Denitrification. In *Comprehensive Coordination Chemistry II: Bio-Coordination Chemistry* (Que, L. T. W., Ed.) Vol. 8, pp 759−786, Elsevier, Oxford, U.K.
3. Antonyuk, S. V., Strange, R. W., Sawers, G., Eady, R. R., and Hasnain, S. S. (2005) Atomic resolution structures of resting-state, substrate- and product-complexed Cu-nitrite reductase provide insight into catalytic mechanism. *Proc. Natl. Acad. Sci. U.S.A. 102*, 12041–12046.
4. Hough, M. A., Ellis, M. J., Antonyuk, S., Strange, R. W., Sawers, G., Eady, R. R., and Hasnain, S. S. (2005) High resolution structural studies of mutants provide insights into catalysis and electron transfer processes in copper nitrite reductase. *J. Mol. Biol. 350*, 300–309.
5. Strange, R. W., Murphy, L. M., Dodd, F. E., Abraham, Z. H. L., Eady, R. R., Smith, B. E., and Hasnain, S. S. (1999) Structural and kinetic evidence for an ordered mechanism of copper nitrite reductase. *J. Mol. Biol. 287*, 1001–1009.
6. Wijma, H. J., Jeuken, L. J. C., Verbeet, M. P., Armstrong, F. A., and Canters, G. W. (2006) A random-sequential mechanism for nitrite binding and active site reduction in copper-containing nitrite-reductase. *J. Biol. Chem. 281*, 16340–16346.
7. Dodd, F. E., Van Beeumen, J., Eady, R. R., and Hasnain, S. S. (1998) X-ray structure of a blue-copper nitrite reductase in two crystal forms. The nature of the copper sites, mode of substrate binding and recognition by redox partner. *J. Mol. Biol. 282*, 369–382.
8. Ellis, M. J., Dodd, F. E., Strange, R. W., Prudencio, M., Sawers, G., Eady, R. R., and Hasnain, S. S. (2001) X-ray structure of a blue copper nitrite reductase at high pH and in copper-free form at 1.9 Å resolution. *Acta Crystallogr. D57*, 1110–1118.
9. Ellis, M. J., Dodd, F. E., Sawers, G., Eady, R. R., and Hasnain, S. S. (2003) Atomic resolution structures of native copper nitrite reductase from *Alcaligenes xylosoxidans* and the active site mutant Asp92Glu. *J. Mol. Biol. 328*, 429–438.
10. Ellis, M. J., Prudencio, M., Dodd, F. E., Strange, R. W., Sawers, G., Eady, R. R., and Hasnain, S. S. (2002) Biochemical and crystallographic studies of the Met144Ala, Asp92Asn and His254Phe mutants of the nitrite reductase from *Alcaligenes xylosoxidans* provide insight into the enzyme mechanism. *J. Mol. Biol. 316*, 51–64.
11. Abraham, Z. H. L., Lowe, D. J., and Smith, B. E. (1993) Purification and characterisation of the dissimilatory nitrite reductase from *Alcaligenes xylosoxidans* subsp *xylosoxidans* (NCIMB 11015): Evidence for the presence of both type 1 and type 2 copper centres. *Biochem. J. 295*, 587–593.
12. Hough, M. A., Antonyuk, S. V., Strange, R. W., Eady, R. R., and Hasnain, S. S. (2008) Crystallography with online optical and X-ray absorption spectroscopies demonstrates an ordered mechanism in copper nitrite reductase. *J. Mol. Biol. 378*, 353–361.
13. Prudencio, M., Eady, R. R., and Sawers, G. (1999) The blue copper-containing nitrite reductase from *Alcaligenes xylosoxidans*: Cloning of the nirA gene and characterization of the recombinant enzyme. *J. Bacteriol. 181*, 2323–2329.
14. Cianci, M., Antonyuk, S., Bliss, N., Bailey, M. W., Buffey, S. G., Cheung, K. C., Clarke, J. A., Derbyshire, G. E., Ellis, M. J., Enderby, M. J., Grant, A. F., Holbourn, M. P., Laundy, D., Nave, C., Ryder, R., Stephenson, P., Helliwell, J. R., and Hasnain, S. S. (2005) A high-throughput structural biology/proteomics beamline at the SRS on a new multipole wiggler. *J. Synchrotron Radiat. 12*, 455–466.
15. McCoy, A. J., Grosse-Kunstleve, R. W., Adams, P. D., Winn, M. D., Storoni, L. C., and Read, R. J. (2007) Phaser crystallographic software. *J. Appl. Crystallogr. 40*, 658–674.
16. Murshudov, G. N., Vagin, A. A., and Dodson, E. J. (1997) Refinement of macromolecular structures by the maximum-likelihood method. *Acta Crystallogr. D53*, 240–255.
17. Winn, M. D., Murshudov, G. N., and Papiz, M. Z. (2003) Macromolecular TLS refinement in REFMAC at moderate resolutions. *Methods Enzymol. 374*, 300–321.
18. Emsley, P., and Cowtan, K. (2004) Coot: Model-building tools for molecular graphics. *Acta Crystallogr. D60*, 2126–2132.
19. Laskowski, R. A., MacArthur, M. W., Moss, D. S., and Thornton, J. M. (1993) PROCHECK: A program to check the stereochemical quality of protein structures. *J. Appl. Crystallogr. 26*, 283–291.
20. Abraham, Z. H. L., Smith, B. E., Howes, D., Lowe, D. J., and Eady, R. R. (1997) pH dependence for binding a single nitrite ion to each type-2 copper centre in the copper-containing nitrite reductase from *Alcaligenes xylosoxidans*. *Biochem. J. 324*, 511–516.

BI801369Y